

## Optimal design of bio-inspired isolation systems using performance and fragility objectives

Fan Hu<sup>1,2a</sup>, Zhiguo Shi<sup>1b</sup> and Jiazeng Shan<sup>\*1</sup>

<sup>1</sup>Research Institute of Structural Engineering and Disaster Reduction, Tongji University, Shanghai 200092, China

<sup>2</sup>Department of Civil and Environmental Engineering, University of California, Berkeley CA, 94704, United States

(Received February 28, 2018, Revised July 13, 2018, Accepted July 19, 2018)

**Abstract.** This study aims to propose a performance-based design method of a novel passive base isolation system, BIO isolation system, which is inspired by an energy dissipation mechanism called ‘sacrificial bonds and hidden length’. Fragility functions utilized in this study are derived, indicating the probability that a component, element, or system will be damaged as a function of a single predictive demand parameter. Based on PEER framework methodology for Performance-Based Earthquake Engineering (PBEE), a systematic design procedure using performance and fragility objectives is presented. Base displacement, superstructure absolute acceleration and story drift ratio are selected as engineering demand parameters. The new design method is then performed on a general two degree-of-freedom (2DOF) structure model and the optimal design under different seismic intensities is obtained through numerical analysis. Seismic performances of the biologically inspired (BIO) isolation system are compared with that of the linear isolation system. To further demonstrate the feasibility and effectiveness of this method, the BIO isolation system of a 4-storey reinforced concrete building is designed and investigated. The newly designed BIO isolators effectively decrease the superstructure responses and base displacement under selected earthquake excitations, showing good seismic performance.

**Keywords:** bio-inspired isolator; seismic performance; fragility; optimal design

### 1. Introduction

In recent decades, base isolation has aroused great interest among researchers and engineers due to the excellent control ability of structural seismic response. Base isolation denotes decoupling a superstructure from its substructure by setting a flexible isolation layer, which therefore, changes the fundamental frequency of the structure and significantly reduces the seismic energy transferred to the structure (Skinner *et al.* 1993). In mid 1960s, base isolation emerged as a new technology in Japan, the United States, and some other earthquake-prone areas, and large quantities of systematic theoretical and experimental research have been conducted since then.

---

\*Corresponding author, Associate Professor, E-mail: [jzshan@tongji.edu.cn](mailto:jzshan@tongji.edu.cn)

<sup>a</sup> Graduate Student, E-mail: [fan\\_hu@berkeley.edu](mailto:fan_hu@berkeley.edu)

<sup>b</sup> Ph.D. Student, E-mail: [shizhiguo@tongji.edu.cn](mailto:shizhiguo@tongji.edu.cn)

Over the years, base isolation technology has proven to be a cost-effective and reliable strategy for mitigating seismic damage to structures (Kelly 1997).

It has been found that for near-fault motions an isolated structure with conventional passive isolators may suffer from undue base displacement (Jangid and Kelly 2001, Nagarajaiah *et al.* 2008). The addition of damping to control base displacement, however, will probably intensify the responses of the superstructure. Recently, passive isolation systems with innovative technologies have gradually drawn researchers' attention. One of the innovative passive base isolation systems regarding to our research is BIO isolation system (Yang *et al.* 2010, Chen *et al.* 2016), which is inspired by an energy dissipation mechanism called 'sacrificial bonds and hidden length'. Chen *et al.* (2016) have proposed a response-based optimal design procedure for the bio-inspired isolator based on a multi-objective optimization approach. Recently, a novel nonlinear isolation system has been numerically investigated, a stochastic response evaluation has been employed and a small-scale preliminary prototype has been experimentally studied (Shan *et al.* 2018).

Researchers have proposed various optimization methods of base isolation systems. Moeindarbari and Taghikhany (2014) have applied a specific numerical optimization method based on Genetic Algorithms to determine the optimum values of the design variables that minimize superstructure demands. Kim *et al.* (2006) have proposed a multi-objective genetic algorithm for a fuzzy logic controller (FLC), which is used to optimize parameters of membership functions and find appropriate fuzzy rules. Scruggs *et al.* (2006) have proposed a probability-based active control synthesis for seismic base isolation of a structure subjected to uncertain future ground motions, in which the performance objective is the minimization of the probability of failure.

The main objective of the current study is to present an optimal design for bio-inspired isolation systems that meets desired performance targets. Performance-Based Earthquake Engineering (PBEE) is defined as design and evaluation for the achievement of specified results rather than prescribed means (May 2003). PEER framework for PBEE involves four steps: seismic hazard analysis, structural demand analysis, fragility analysis and loss analysis. Seismic fragility refers to the probability that a structure or a component suffers damage under earthquake of different intensities, which quantitatively depicts the seismic performance of a structure or a component. In the 1970s, the National Oceanic and Atmospheric Administration (NOAA) and the United States Geological Survey (USGS) investigated loss estimation in seismic events in Los Angeles and San Francisco, and established NOAA/USGS method to characterize the earthquake-damage relation, which is often used in regional seismic loss estimation. In the 1980s, the Federal Emergency Management Agency (FEMA) commissioned the Applied Technology Council (ATC) to propose a practical method of seismic damage estimation, resulting in the ATC-13 method. This method was derived from experts' experience and provided the damage probability of a building under earthquakes of different intensities.

This paper elaborates on an optimal design approach of a biologically inspired passive isolation system using performance and fragility objectives. First, a brief introduction of the bio-inspired isolated structural system is presented. Then the fragility functions utilized in our study are derived, and a systematic performance-based design method of bio-inspired isolation systems is proposed. Next, a two degree-of-freedom (2DOF) isolated structure model is constructed and numerical analysis of the structure under a series of ground motions is used to illustrate the new optimal design method. Finally, the new optimal design method is applied to design the BIO isolation system for a 4-storey reinforced concrete building, the seismic performance of which is evaluated to further prove the presented theory.

## 2. Design framework

### 2.1 Bio-inspired isolator

Chen *et al.* (2016) proposed a biologically inspired passive isolation system, which integrates a conventional linear isolator with an energy dispersion mechanism called sacrificial bonds and hidden length (Hansma *et al.* 2005). The mechanical model of the bio-inspired isolator is conceptually illustrated in Fig. 1.

The restoring force predicted by the model is given by

$$f_{\text{BIO}}(x, \dot{x}) = k_b x + c_b \dot{x} + \text{BIO}(x, \dot{x}) \tag{1}$$

where  $x$  and  $\dot{x}$  are the displacement and velocity of the isolator,  $k_b$  and  $c_b$  are the stiffness and damping coefficients of the isolator, respectively, and  $\text{BIO}(x, \dot{x})$  is the bio-inspired force component, which was defined in a piecewise function form (Yang *et al.* 2010),

$$\text{BIO}(x, \dot{x}) = \begin{cases} f_{\text{max}} & \text{if } x \geq 0 \text{ and } \dot{x} \leq 0 \\ -f_{\text{max}} & \text{if } x \leq 0 \text{ and } \dot{x} \geq 0 \\ 0 & \text{if } x \cdot \dot{x} > 0 \end{cases} \tag{2}$$

where  $f_{\text{max}}$  is the maximum force assumed in the sacrificial bonds and hidden length mechanism.

### 2.2 Fragility function

Fragility function in earthquake engineering expresses the probability that the seismic demand of a component or a structure exceeds its capacity as a function of seismic intensity.

$$P_f = P\left(\frac{S_d}{S_c} \geq 1\right) \tag{3}$$

where  $P_f$  is the probability that a component or a structure reaches or exceeds some limit state,  $P(A)$  is the probability that  $A$  occurs,  $S_d$  is the seismic demand of a component or a structure (e.g., story drift ratio, floor acceleration),  $S_c$  is the seismic capacity of a component or a structure.

The most common form of a seismic fragility function is the lognormal cumulative distribution function. It is of the form

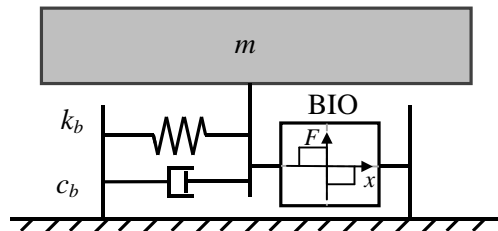


Fig. 1 Simple mechanical model of the bio-inspired isolator

$$F_i(D) = \Phi\left(\frac{\ln(S_d / \theta_i)}{\beta_i}\right) \quad (4)$$

where  $F_i(D)$  is a fragility function for damage state  $i$  evaluated at  $D$ ,  $D$  represents engineering demand parameter,  $S_d$  is a particular value of  $D$ ,  $\Phi$  is the standard normal cumulative distribution function,  $\theta_i$  is the median value of the seismic capacity to resist damage state  $i$ ,  $\beta_i$  is the logarithmic standard deviation of the seismic capacity to resist damage state  $i$ .

The relation between Engineering Demand Parameter ( $S_d$ ) and Intensity Measure ( $PGA$ ) can be described as (Mackie 2005)

$$S_d = a(PGA)^b \quad (5)$$

where  $a, b$  are constants.

Changing to the logarithmic form

$$\ln(S_d) = A \ln(PGA) + B \quad (6)$$

where  $A, B$  are constants obtained by regression analysis of response simulations.

Combining the above relations

$$P_f = F_i(D) = \Phi\left(\frac{A \ln(PGA) + B - \ln \theta_i}{\beta_i}\right) \quad (7)$$

Eq. (7) is the fragility function utilized in our study.

### 2.3 Damage state

According to FEMA (2012), damage is characterized as a series of discrete damage states representing the different levels of possible damage. Each damage state represents a unique set of consequences (e.g., a unique repair cost). Using this principle, three damage states are adopted in our study, as shown in Table 1.

Table 1 Description of three damage states

Damage State	Damage Level	Function Description	Repairing After Earthquake
DS1	minor damage	Not or slightly disturbed: without structural damage but possibly some nonstructural damage; without risk to public health and safety	No repairing required or only surface repairing required
DS2	moderate damage	Moderately disturbed: with some structural and nonstructural damage; without risk to public health and safety, but not suitable to live in the short term after an earthquake	Repairable, replacement of some components required, causing considerable economic losses
DS3	severe damage	Severely or completely disturbed: with severe structural and nonstructural damage; with high risk to public safety	Not repairable either technically or economically, entire replacement required

Table 2 Symbols for the median value and the logarithmic standard deviation of the seismic capacity to resist three damage states

Damage State	Median Value	Logarithmic Standard Deviation
DS1	$\theta_1$	$\beta_1$
DS2	$\theta_2$	$\beta_2$
DS3	$\theta_3$	$\beta_3$

Table 3 Median values and logarithmic standard deviations of the seismic capacity to resist three damage states evaluated at different EDPs

Engineering Demand Parameter	Damage State	$\theta_i$	$\beta_i$
base displacement $x_b$	DS1	0.15 (m)	0.5
	DS2	0.225 (m)	0.5
	DS3	0.30 (m)	0.5
superstructure absolute acceleration $a_s$	DS1	0.375 (g)	0.8
	DS2	0.75 (g)	0.8
	DS3	1.50 (g)	0.8
story drift ratio $\Delta$	DS1	1/250	0.7
	DS2	1/125	0.7
	DS3	1/40	0.7

We use different symbols to represent the median value and the logarithmic standard deviation of the seismic capacity to resist three damage states, as shown in Table 2.

A performance group is a collection of similar components with identical earthquake demands. For the design of an isolation system, base displacement is an important parameter. Researchers have shown that in real earthquakes, the damage of nonstructural components is much more severe than that of structural components, and the nonstructural components can be divided into acceleration-sensitive components and displacement-sensitive components (Taghavi and Miranda 2003). Therefore, in this paper, base displacement  $x_b$ , superstructure absolute acceleration  $a_s$ , story drift ratios  $\Delta$  are chosen as the engineering demand parameters (EDPs) of bio-inspired isolation systems. The selected median values and logarithmic standard deviations of the seismic capacity to resist three damage states evaluated at different EDPs are listed in Table 3 separately (FEMA 2012, Kaynia *et al.* 2013).

#### 2.4 Systematic performance-based design method

According to the framework and methodology for PBEE and the nonlinear dynamic analysis results of bio-inspired isolation systems, we propose a systematic performance-based design method of bio-inspired isolation systems, which includes the following steps:

- (1) Divide the structural and nonstructural components into several performance groups (PGs),

- with a seismic engineering demand parameter  $D$  for a corresponding performance group.
- (2) Select appropriate suites of earthquake ground motions.
  - (3) Set the initial value of the bio-inspired force ratio in the isolation system as  $\eta_0$ , and then construct the bio-isolated structure model using Matlab/Simulink.
  - (4) Perform response history analysis using the selected ground motions to get all relevant EDP values ( $S_d$ ).
  - (5) Perform logarithmic linear regression to get  $\ln(S_d) = A \ln(PGA) + B$  (where  $A$ ,  $B$  are constants).
  - (6) Construct the seismic fragility function evaluated at  $D$

$$P_f = \Phi\left(\frac{A \ln(PGA) + B - \ln \theta}{\beta}\right)$$

- (7) Calculate the seismic fragility of the bio-isolated structure  $P_f(pga)$  for a given earthquake intensity  $pga$ .
- (8) Change the value of the bio-inspired force ratio  $\eta$  and repeat (3) - (7).
- (9) Analyze the relation between the system parameter  $\eta$  and the seismic fragility  $P_f(pga)$ , then the optimal bio-inspired force ratio  $\eta$  corresponds to the minimum value of  $P_f(pga)$ .

### 3. Illustrative example

#### 3.1 Two degree-of-freedom (2DOF) lumped model

In our study, a two degree-of-freedom (2DOF) isolated structure model is adopted, which includes the bio-inspired isolation system and the superstructure (Ramallo *et al.* 2002). The governing equation of motion can be written as

$$\begin{aligned} & \begin{bmatrix} 1-\gamma & 0 \\ 0 & 1 \end{bmatrix} \begin{Bmatrix} \ddot{x}_b \\ \ddot{x}_s \end{Bmatrix} + \begin{bmatrix} 2\xi_b \omega_b + 2\gamma \xi_s \omega_s & -2\gamma \xi_s \omega_s \\ -2\xi_s \omega_s & 2\xi_s \omega_s \end{bmatrix} \begin{Bmatrix} \dot{x}_b \\ \dot{x}_s \end{Bmatrix} + \begin{bmatrix} \omega_b^2 + \gamma \omega_s^2 & -\gamma \omega_s^2 \\ -\omega_s^2 & \omega_s^2 \end{bmatrix} \begin{Bmatrix} x_b \\ x_s \end{Bmatrix} \\ & = \begin{Bmatrix} \text{BIO}(x_b, \dot{x}_b) \\ 0 \end{Bmatrix} g - \begin{bmatrix} 1-\gamma & 0 \\ 0 & 1 \end{bmatrix} \begin{Bmatrix} 1 \\ 1 \end{Bmatrix} \ddot{x}_g \end{aligned} \quad (8)$$

$\xi_b$  is the damping ratio of the isolator,  $\xi_s$  is the damping ratio of the structure. The proposed bio-inspired force ratio  $\eta$  is defined as  $f_{\max}/W$ , where  $W$  is the total weight of the isolated building structure. The mass ratio  $\gamma$  is  $m_s/(m_s+m_b)$ .

To obtain a reasonable design of the bio-inspired isolator, the influences of the stiffness  $k_b$ , damping  $c_b$ , and bio-inspired force component  $\text{BIO}(x, \dot{x})$  on the isolation performance will be considered. According to Eq. (8), the bio-inspired force component  $\text{BIO}(x, \dot{x})$  depends on  $f_{\max}$ . In this study, we focus on the influence of the bio-inspired force ratio  $\eta = f_{\max}/W$ .

We use some of the optimization results by Chen *et al.* (2016), which include the natural periods  $T_b$  and  $T_s$ , the damping ratios  $\xi_b$  and  $\xi_s$ . The default values of the properties of the adopted 2DOF isolated structural model, and the assumed range of variation of the studied parameter  $\eta$  are presented in Table 4. When  $\eta=0$ , the studied bio-inspired isolation system becomes a conventional linear isolation system, which can be used for comparison.

Table 4 Values of the parameters for the superstructure and the isolation system of the 2DOF bio-isolated structural model

Superstructure	Isolation System	
	Linear Isolation	Bio-inspired Isolation
$T_s = 0.135 \text{ sec}$	$T_b = 2.5 \text{ sec}$	$T_b = 2.5 \text{ sec}$
$\xi_s = 2\%$	$\xi_b = 5\%$	$\xi_b = 5\%$
$\gamma = 0.8$	$\eta = 0$	$\eta = 0.01 : 0.01 : 0.1$
$m_s = 29485 \text{ kg}$		$m_b = 6800 \text{ kg}$
$k_s = 1.1912 \times 10^7 \text{ N/m}$		$k_b = 2.32 \times 10^5 \text{ N/m}$
$c_s = 23710 \text{ N*s/m}$		$c_b = 9116.4 \text{ N*s/m}$

Table 5 Ground motion records

NO#	RSN	Event	Motion Name	Peak Ground Acceleration (PGA) / (m/sec <sup>2</sup> )	Predominant Period / sec	Duration / sec
1	50	LYTLECR	WTW115	1.416	0.26	3.2
2	147	COYOTELK	G02050	1.870	0.18	7.5
3	149	COYOTELK	G04360	2.466	0.32	11
4	158	IMPVALL.H	H-AEP045	3.007	0.1	9.8
5	160	IMPVALL.H	H-BCR230	7.614	0.38	9.7
6	174	IMPVALL.H	H-E11140	3.595	0.24	9
7	174	IMPVALL.H	H-E11230	3.718	0.26	9
8	180	IMPVALL.H	H-E05140	5.181	0.34	9.6
9	182	IMPVALL.H	H-E07140	3.340	0.7	6.8
10	185	IMPVALL.H	H-HVP225	2.530	0.34	12.8
11	185	IMPVALL.H	H-HVP315	2.170	0.22	12.8
12	202	IMPVALL.A	A-E04140	2.293	0.18	7.6
13	202	IMPVALL.A	A-E04230	1.622	0.36	7.6
14	452	MORGAN	A01310	0.635	0.3	35.7
15	524	PALMSPR	JOS090	0.639	0.16	17.5
16	659	WHITTIER.A	A-WPA060	0.439	0.18	16.9
17	762	LOMAP	FRE090	1.038	0.18	18.2
18	768	LOMAP	G04090	2.121	0.54	14.8
19	828	CAPEMEND	PET000	5.790	0.66	17.7
20	952	NORTHR	MU2035	6.085	0.26	7.7

Continued-

21	959	NORTHR	CNP196	3.840	0.6	11.9
22	961	NORTHR	CAT090	0.953	0.4	21
23	961	NORTHR	CAT-UP	0.475	0.2	21
24	985	NORTHR	BLD090	2.341	0.28	17.3
25	987	NORTHR	CEN245	3.121	0.14	12.2
26	997	NORTHR	FIG058	1.300	0.26	13.1
27	997	NORTHR	FIG328	1.611	0.18	13.1
28	1004	NORTHR	SPV270	7.375	0.66	8.5
29	1107	KOBE	KAK000	2.355	0.16	13.2
30	1107	KOBE	KAK090	3.177	0.16	13.2
31	1116	KOBE	SHI000	2.205	0.66	11.6
32	1119	KOBE	TAZ090	6.016	0.48	4.6
33	1158	KOCAELI	DZC180	3.057	0.38	11.8
34	1158	KOCAELI	DZC270	3.569	0.28	11.8
35	1602	DUZCE	BOL090	7.896	0.36	9

To perform response history analysis of the bio-isolated structure model, 35 ground motion records are selected as the excitation, the detailed information is shown in Table 5.

### 3.2 Relations between fragility and bio-inspired force ratio

#### 3.2.1 Fragility evaluated by base displacement $x_b$

First, we input the selected 35 earthquake records as excitation and get the base displacements of the 2DOF model under different earthquake intensities by numerical simulations.

Using logarithmic linear regression to analyze the relation between base displacements and peak ground accelerations, we obtain

$$\ln(x_{bi}) = A_i \ln(PGA) + B_i \quad (9)$$

where  $A_i$  and  $B_i$  are constants corresponding to different  $\eta_i$ .

The fragility functions for three damage states evaluated by base displacement are

$$P_{f1i} = \Phi \left( \frac{A_i \ln(PGA) + B_i - \ln(0.15)}{0.5} \right) \quad (10.1)$$

$$P_{f2i} = \Phi \left( \frac{A_i \ln(PGA) + B_i - \ln(0.225)}{0.5} \right) \quad (10.2)$$

$$P_{f3i} = \Phi \left( \frac{A_i \ln(PGA) + B_i - \ln(0.30)}{0.5} \right) \quad (10.3)$$

Table 6 Logarithmic linear regression analysis results

$i$	$\eta_i$	$A_i$	$B_i$
1	0	1.2488	-3.4572
2	0.01	1.2194	-3.5679
3	0.02	1.0486	-3.3991
4	0.03	0.8744	-3.2245
5	0.04	0.7516	-3.0829
6	0.05	0.6468	-2.9221
7	0.06	0.5672	-2.8127
8	0.07	0.5181	-2.7195
9	0.08	0.4588	-2.6208
10	0.09	0.415	-2.5457
11	0.1	0.3679	-2.4589

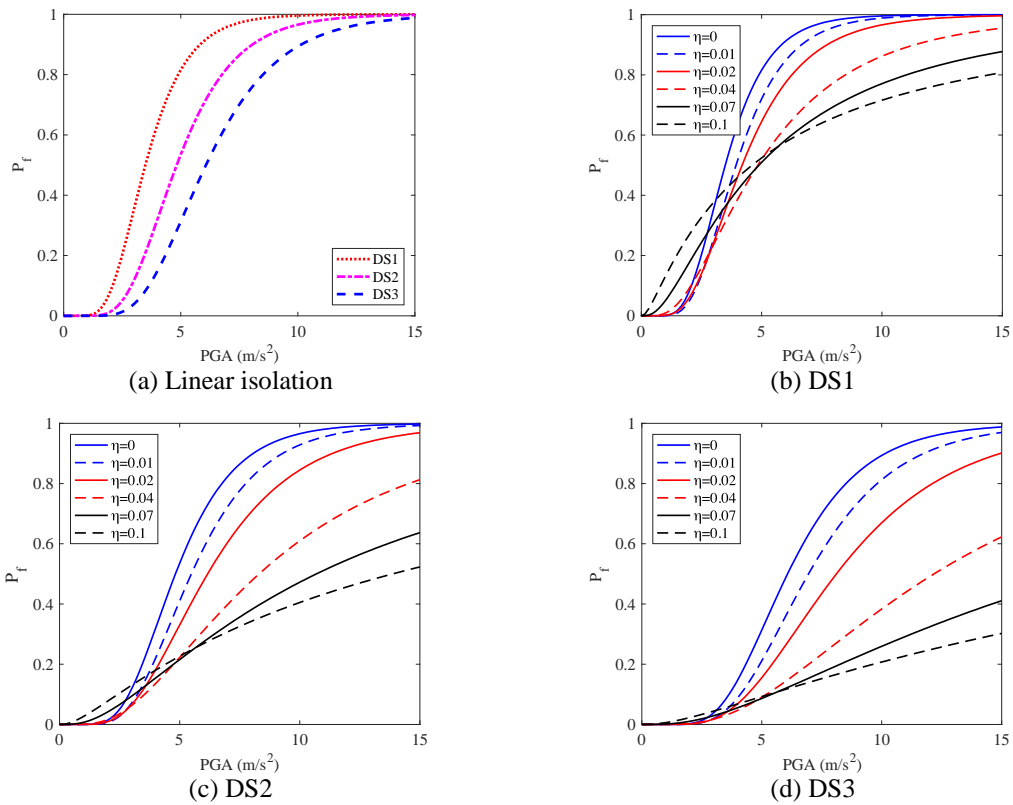


Fig. 3 Fragility curves (evaluated by base displacement) for the linear isolation system and the BIO isolation system with different bio-inspired force ratios

The fragility curves for the linear isolation system and the BIO isolation system with  $\eta = 0, 0.01, 0.02, 0.04, 0.07, 0.10$  under different damage states are shown in Fig. 3. For the linear isolation system in Fig. 3 (a), when the damage state gets more severe, the corresponding fragility curve becomes lower in the graph, which suggests that the damage is less likely to happen. Fig. (b)-(d) correspond to the BIO isolation system under three damage states respectively, with each figure showing the system with changing  $\eta$  under one damage state. The relative position of two curves indicates the comparison of the seismic fragilities of two different BIO isolation systems. For a specific damage state, the smallest fragility corresponds to different system parameter  $\eta$  under different seismic intensity measures. As such, we first select a general PGA which equals to  $4 \text{ m/s}^2$  to investigate the optimal value of  $\eta$ .

When PGA equals to  $4 \text{ m/s}^2$ , the fragilities of the bio-isolated structure in three damage states are calculated. And therefore, the relations between the seismic fragility and the bio-inspired force ratio can be attained.

It is suggested that when  $\text{PGA} = 4 \text{ m/s}^2$ , the fragility curves reach their minimum values at  $\eta = 0.04$  for all three damage states, which indicates that  $\eta = 0.04$  is the optimal design case of the bio isolation system when  $\text{PGA} = 4 \text{ m/s}^2$ .

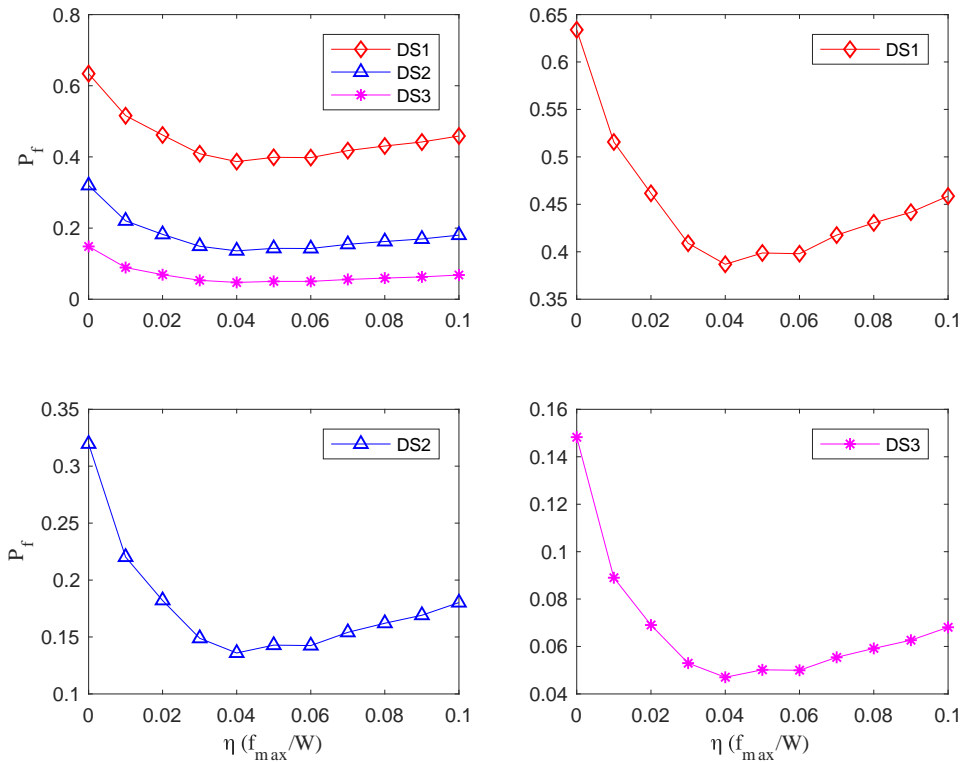


Fig. 4 Relation between the seismic fragility evaluated by  $x_b$  and bio-inspired force ratio  $\eta$  (PGA =  $4 \text{ m/s}^2$ )

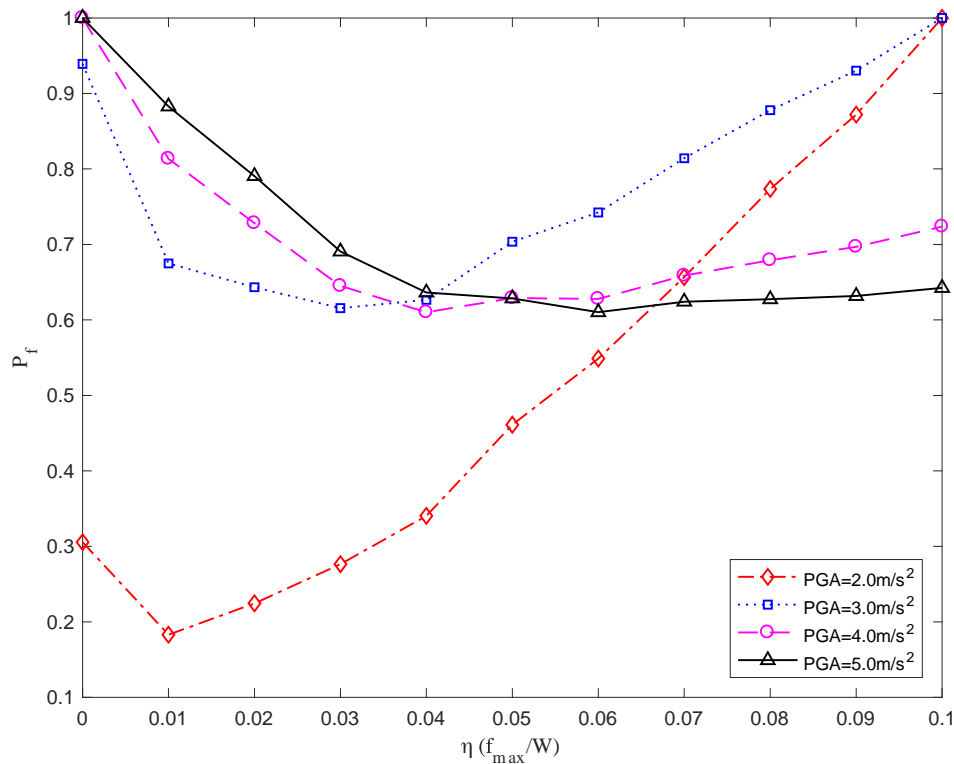


Fig. 5 Relation between the normalized DS1 seismic fragility evaluated by  $x_b$  and bio-inspired force ratio  $\eta$

Similarly, we can obtain such relations when PGA equals 2 m/s<sup>2</sup>, 3 m/s<sup>2</sup> and 5 m/s<sup>2</sup>. Since the relations between  $P_f$  and  $\eta$  are close to each other for three damage states at a particular earthquake intensity, we only consider DS1.

When seismic intensity measure increases, the isolated structure becomes more vulnerable to damage. Therefore, each  $P_f - \eta$  curve is normalized through dividing each fragility value by the maximum fragility on that curve. After normalization, we are able to compare the relations at different PGAs in one figure. From Fig. 5, when PGA = 2 m/s<sup>2</sup>,  $\eta = 0.01$  is the optimal design case; when PGA = 3 m/s<sup>2</sup>,  $\eta = 0.03$  is the optimal design case; when PGA = 4 m/s<sup>2</sup>,  $\eta = 0.04$  is the optimal design case; when PGA = 5 m/s<sup>2</sup>,  $\eta = 0.06$  is the optimal design case. Clearly, when the fragility is evaluated by the base displacement, the optimal value of bio-inspired force ratio gets larger as PGA increases. As such, for different seismic intensity measures, we may find the optimal design value of the BIO isolation system for the 2DOF structural model.

### 3.2.2 Fragility evaluated by superstructure absolute acceleration $a_s$

For acceleration sensitive components, the fragility is evaluated by the superstructure absolute acceleration  $a_s$ . We perform the same design procedure and get the relation between the normalized DS1 seismic fragility evaluated by  $a_s$  and  $\eta$ . From Fig. 6, when PGA = 2 m/s<sup>2</sup>,  $\eta = 0$

is the optimal design case (i.e., the linear isolation); when  $\text{PGA} = 3 \text{ m/s}^2$ ,  $\eta = 0.01$  is the optimal design case; when  $\text{PGA} = 4 \text{ m/s}^2$ ,  $\eta = 0.02$  is the optimal design case; when  $\text{PGA} = 5 \text{ m/s}^2$ ,  $\eta = 0.04$  is the optimal design case.

It is obvious that when the fragility is evaluated by the superstructure absolute acceleration, the optimal value of bio-inspired force ratio increases as PGA increases. However, for any specific seismic intensity measure, the optimal design value of  $\eta$  varies between the case evaluated by base displacement and superstructure absolute acceleration. And these factors need to be taken into account when optimizing the design of BIO isolation system of a particular structure.

### 3.2.3 Fragility evaluated by story drift ratio $\Delta$

We perform the same design procedure and get the relation between the normalized DS1 seismic fragility evaluated by  $\Delta$  and  $\eta$ . From Fig. 7, when  $\text{PGA} = 2 \text{ m/s}^2$ ,  $\eta = 0$  is the optimal design case (i.e., the linear isolation); when  $\text{PGA} = 3 \text{ m/s}^2$ ,  $\eta = 0.01$  is the optimal design case; when  $\text{PGA} = 4 \text{ m/s}^2$ ,  $\eta = 0.02$  is the optimal design case; when  $\text{PGA} = 5 \text{ m/s}^2$ ,  $\eta = 0.04$  is the optimal design case.

When the fragility is evaluated by the story drift ratio, the optimal value of bio-inspired force ratio evidently increases with growing PGA. By comparison, we reach that the case evaluated by the story drift ratio shows great similarity to the case evaluated by the superstructure absolute acceleration.

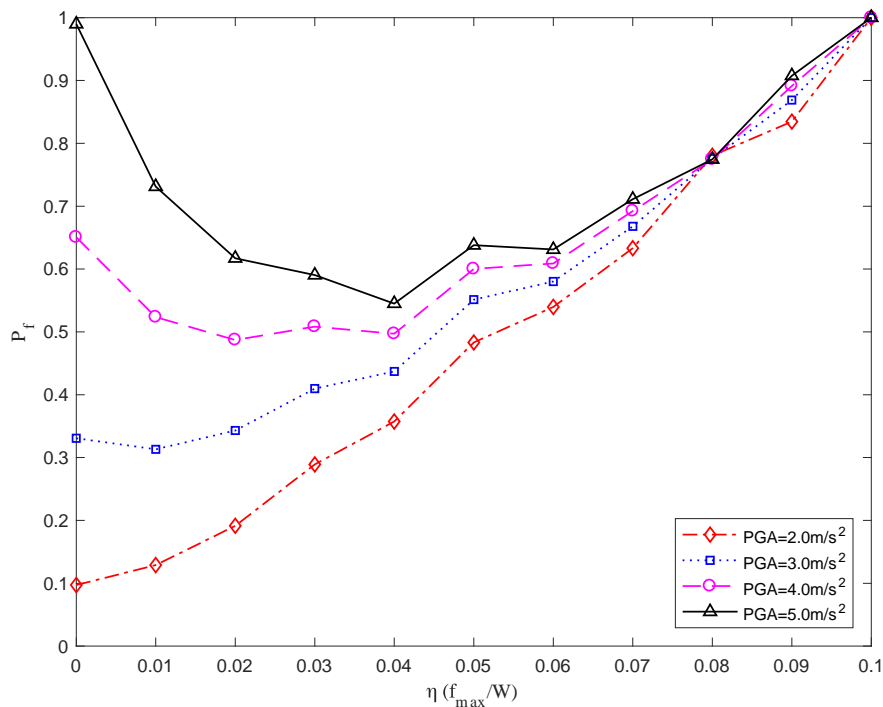


Fig. 6 Relation between the normalized DS1 seismic fragility evaluated by  $a_s$  and bio-inspired force ratio  $\eta$

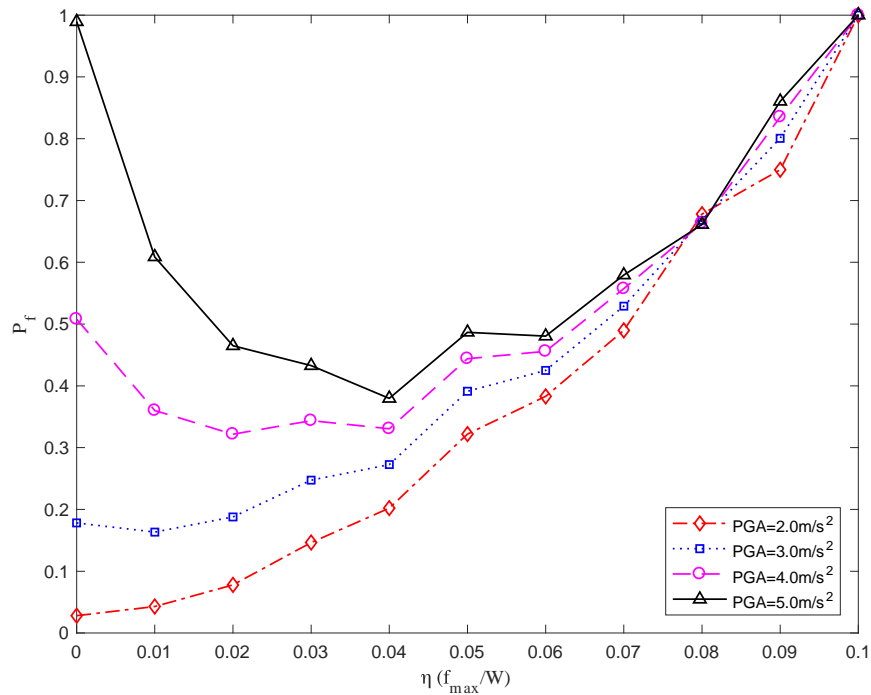


Fig. 7 Relation between the normalized DS1 seismic fragility evaluated by  $\Delta$  and bio-inspired force ratio  $\eta$

### 3.3 Comparisons with response-based optimal design

The response-based optimal design emphasizes on meeting certain criteria in the codes, with structural performance as an unexpected consequence of design. And therefore, the performance, damage, financial loss cannot be expected quantitatively. Besides, designers focus on structural components rather than non-structural components that may cause larger financial loss.

However, for the new optimal design, designers use structural performance and fragility as the design objectives, which allows the requirements in seismic codes to be understood quantitatively. Besides, both structural and non-structural components are taken into account, making the new optimal design method more reasonable.

## 4. Engineering case analysis

### 4.1 Project overview

To further corroborate the theory of optimal design proposed above, we designed the BIO isolation system for a 4-storey bio-isolated reinforced concrete building by applying the new design method.

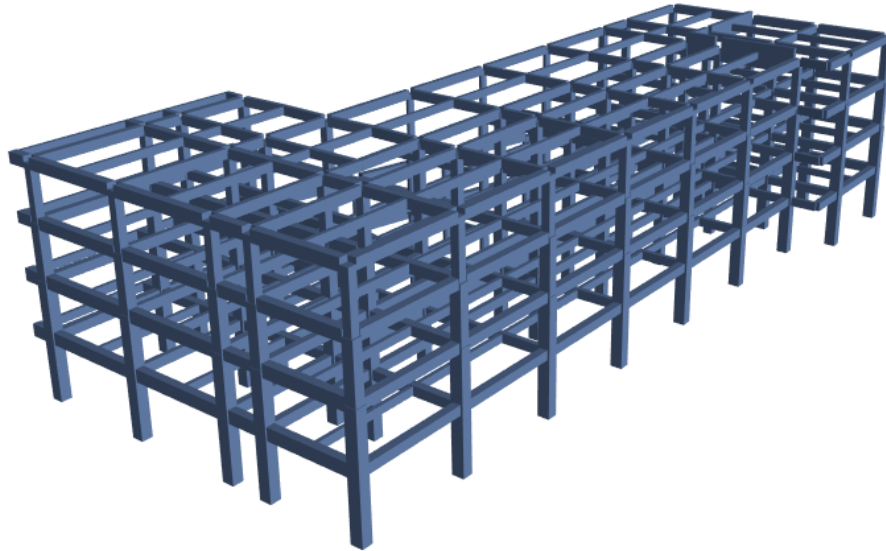


Fig. 8 3D ETABS model of the 4-storey building

This 4-storey building is a teaching building in a primary school without basement, with the length of 64.4 m, the width of 27.2 m, the gross floor area of 6024 m<sup>2</sup>, and the height of 16.6 m.

The superstructure is reinforced concrete frame structure. The modified basic wind pressure is 0.30kN/m<sup>2</sup>. The surface roughness category is C. Only along-wind response is considered and across-wind response is neglected. The structural damping ratio is 0.05. The fundamental natural period of vibration is 0.62s along the X direction and 0.61s along the Y direction.

According to the Chinese Seismic Design Code for Buildings (GB50011-2010), the seismic fortification intensity is 8 degrees, 0.2 g. The maximum earthquake affecting coefficient is 0.16 under frequent earthquakes. The site classification is Class II and the site characteristic period is 0.45s.

A 3D model of this building was established by the finite element software ETABS. The mass distribution of the building is listed in Table 7, and the total mass is 10180873.15 kg.

Table 7 Mass distribution of the 4-storey building

Floor	Mass / (kg)
1	2331623.39
2	2812386.91
3	2502287.07
4	2534575.78

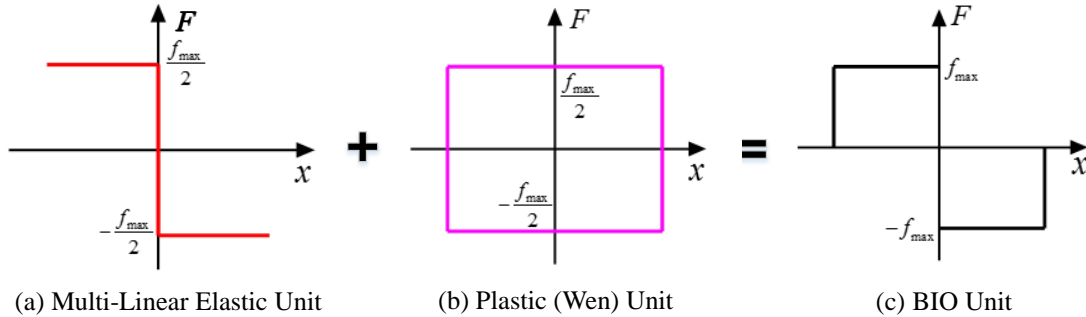


Fig. 9 Force-displacement relation in the BIO Unit in ETABS

Table 8 Values of the parameters for a single isolator used in the 4-storey building

Parameter	Value	Unit
Stiffness	1.85	kN/mm
Damping	56.2	kN*sec/m
BIO Force	85.0	kN

#### 4.2 Fragility-based optimal design of the BIO isolation system

For the isolated structure, the seismic deformations are concentrated on the isolation layer and therefore, the effect of superstructure can be reasonably ignored (Kulkarni and Jangid 2002). Base isolation system essentially changes the fundamental frequency of the structure, thus only the first mode is considered with higher modes being ignored. The fundamental period of the BIO isolated building is approximately 2.5s, which means the results derived from the 2DOF model can be used.

The isolators are arranged separately at the bottom of each column on the ground floor. There are 47 columns in this building, so a total of 47 isolators are needed. Using information from the illustrative 2DOF model, we set  $\eta = 0.004$ . The total mass of the building is 10180873.15 kg, so the total BIO force is 3990.90 kN. Moreover, the total stiffness of the base isolation system is 87.2 kN/mm, and the damping ratio is 5%. Then for a single isolator, the detailed information is shown in Table 8.

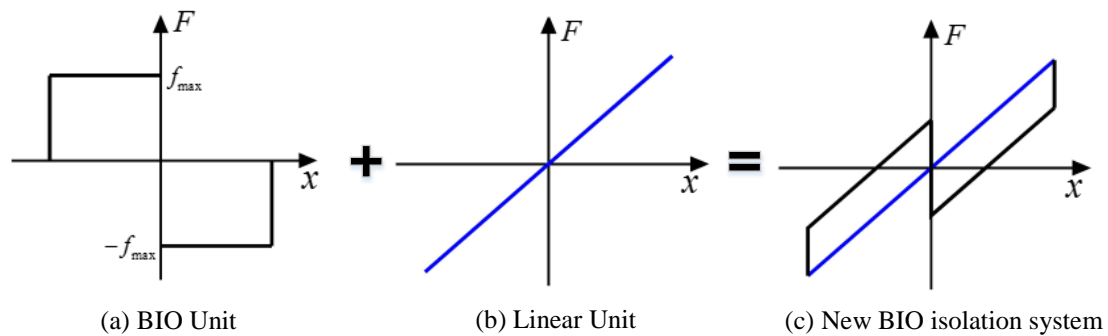


Fig. 10 Force-displacement relation in the new BIO isolation system in ETABS

Table 9 Seismic response of the building under selected ground motions

Floor	Excitation	Without Isolation		With Isolation		Shear Ratio	
		VX/ (kN)	VY/ (kN)	VX/ (kN)	VY/ (kN)	X	Y
4	ChiChi-2966	13552	13527	4988.14	4362.09	0.37	0.32
4	art4	12017	11476	3602.93	3684.32	0.30	0.32
4	San Fernando	13863	14829	4181.77	4987.63	0.30	0.34
3	ChiChi-2966	21956	21279	4788.01	5231.54	0.22	0.25
3	art4	18881	18685	5154.53	5390.89	0.27	0.29
3	San Fernando	22468	22396	6234.41	6240.98	0.28	0.28
2	ChiChi-2966	26980	26965	5255.35	4899.47	0.19	0.18
2	art4	25292	24778	5104.39	5080.06	0.20	0.21
2	San Fernando	29211	29800	5797.13	5556.12	0.20	0.19
1	ChiChi-2966	32317	31432	3529.36	3750.45	0.11	0.12
1	art4	27336	26949	5853.03	5871.08	0.21	0.22
1	San Fernando	31694	32827	6374.70	6448.46	0.20	0.20

In ETABS, we combine the Multi-Linear Elastic Unit and the Plastic (Wen) Unit into a BIO Unit, as shown in Fig. 9. The maximum forces of both the Multi-Linear Elastic Unit and the Plastic (Wen) Unit are set to  $f_{\max}/2$ . Then the new BIO isolation system can be simulated by putting the BIO Unit and the Linear Unit together.

#### 4.3 Performance validation

Two natural and one artificial seismic records are chosen to simulate the seismic response of the bio-isolated structure.

Then the horizontal shear ratio is 0.37 in the X direction and 0.34 in the Y direction, which shows that the designed BIO isolation system has a satisfactory damping effect.

We need to check the deformation capacity of the isolators in rare earthquakes. The peak ground accelerations of three seismic records are adjusted to  $4.0 \text{ m}\cdot\text{sec}^{-2}$ . Then the base displacements of the bio-isolated building under three excitations are simulated separately, as listed in Table 10. The maximum base displacement is 189.2 mm. Nonlinear response history analysis of the original building with rubber isolators under the same excitations suggests that the maximum base displacement is approximately 245 mm, which is much larger than our designed value. And this indicates that the new BIO isolation system has better control effect on base displacement than the conventional base isolation system.

The superstructure absolute accelerations of the bio-isolated building under rare earthquakes are simulated by ETABS. A PGA of  $4.0 \text{ m/s}^2$  is employed. From Table 11, the maximum value is  $2.85 \text{ m/sec}^2$ , which demonstrates that the bio-isolators can effectively decrease the superstructure absolute acceleration.

Table 10 Base displacements of the bio-isolated building under rare earthquakes

Excitation	Base Displacement	
	UX/ (mm)	UY/ (mm)
ChiChi-2966	147.3	145.6
art4	186.5	189.2
San Fernando	176.8	173.8

Table 11 Superstructure absolute accelerations of the bio-isolated building under rare earthquakes

Floor	Excitation	Superstructure Absolute Acceleration	
		X/ (mm·sec <sup>-2</sup> )	Y/ (mm·sec <sup>-2</sup> )
4	ChiChi-2966	2419.28	2667.92
4	art4	2410.63	2350.65
4	San Fernando	2747.09	2795.43
3	ChiChi-2966	2108.94	2298.02
3	art4	2607.87	2762.11
3	San Fernando	2168.19	2423.81
2	ChiChi-2966	1836.13	1835.03
2	art4	1790.54	1760.1
2	San Fernando	1980.03	1855.2
1	ChiChi-2966	2113.69	2344.78
1	art4	2026.8	2062.82
1	San Fernando	<b>2854.24</b>	2678.64

Table 12 Story drift ratios of the bio-isolated building under rare earthquakes

Floor	Excitation	Story Drift Ratio	
		X	Y
4	ChiChi-2966	1/765	1/629
4	art4	1/740	1/660
4	San Fernando	1/682	1/609
3	ChiChi-2966	1/639	1/646
3	art4	1/554	1/559
3	San Fernando	1/562	1/592
2	ChiChi-2966	1/468	1/504
2	art4	1/366	1/407
2	San Fernando	1/407	1/447
1	ChiChi-2966	1/248	1/269
1	art4	<b>1/200</b>	1/211
1	San Fernando	1/216	1/240

The story drift ratios of the bio-isolated building under rare earthquakes are also simulated. The maximum story drift ratio is 1/200, which is much smaller than the allowable value 1/50 (GB50011-2010, 5.5.5) and again shows the effectiveness of our design.

The simulation results of the bio-isolated 4-story building under earthquakes denote that the optimal design method proposed in Chapter 3 is reasonable.

## 5. Conclusions

This paper studies the optimal design of bio-inspired passive isolators using performance and fragility objectives. Based on PEER methodology for PBEE, a systematic design procedure for the new isolation system is proposed and expounded using a 2DOF model. Practical engineering research on a 4-story building is also carried out to evaluate the effectiveness of the optimal performance-based design theory.

According to the dynamic properties of the BIO isolation system, the PEER PBEE framework is explored and an optimal design using performance and fragility objectives is derived theoretically.

The optimal performance-based design procedure is applied to the BIO isolation system of a general 2DOF structure model. Fragility analysis is performed to obtain the optimal bio-inspired force ratio  $\eta$  of the model, with fragility evaluated by base displacement, superstructure absolute acceleration and story drift ratio respectively. When  $\text{PGA} = 4\text{m/s}^2$ , considering three engineering demand parameters,  $\eta = 0.4$  is the optimal design of the BIO isolation system. Selecting a certain seismic intensity, the relations between the seismic fragility and the bio-inspired force ratio can be easily got.

The BIO component can be assembled in ETABS software with Multi-Linear Elastic element and Plastic (Wen) element which are software-provided. The BIO isolation system of a 4-story finite element model is designed by the new optimal design method. Response history analysis of the bio-isolated building under earthquakes indicates that the designed BIO isolation system will effectively diminish the superstructure responses and base displacement, which proves the rationality of the new design method.

In the state-of-the-art seismic study, the fragility is an important index for the earthquake resistance performance evaluation. The proposed design method in current study is an exploration to adopt the fragility concept for base isolation implementation. The next logistical step seems to be compared with other design methods.

## References

- Chen, X., Yang, H.T.Y., Shan, J. et al. (2016), "Bio-inspired passive optimized base-isolation system for seismic mitigation of building structures", *J. Eng. Mech.*, **142**(1), 04015061.
- FEMA, P. (2012), "58-1 seismic performance assessment of buildings (volume 1-methodology)", Federal Emergency Management Agency, Washington.
- Hansma, P.K., Fantner, G.E., Kindt, J.H. et al. (2005), "Sacrificial bonds in the interfibrillar matrix of bone", *J. Musculoskelet Neuronal Interact*, **5**(4), 313-315.
- Jangid, R. and Kelly, J. (2001), "Base isolation for near - fault motions", *Earthq. Eng. Struct. D.*, **30**(5), 691-707.
- Kaynia, A.M., Taucer, F. and Hancilar, U. (2013), Guidelines for deriving seismic fragility functions of

- elements at risk: Buildings, lifelines, transportation networks and critical facilities, Publications Office.
- Kelly, J.M. (1997), Earthquake-resistant design with rubber, Springer London.
- Kim, H.S. and Roschke, P.N. (2006), "Fuzzy control of base-isolation system using multi-objective genetic algorithm", *Comput. Aided Civil Infrastruct. Eng.*, **21**(6), 436-449.
- Kulkarni, J.A. and Jangid, R.S. (2002), "Rigid body response of base-isolated structures", *Struct. Control Health Monit.*, **9**(3), 171-188.
- Mackie, K.R. (2005), Fragility-based seismic decision making for highway overpass bridges.
- May, P.J. (2003), "Performance - based regulation and regulatory regimes: The saga of leaky buildings", *Law & Policy*, **25**(4), 381-401.
- Moeindarbari, H. and Taghikhany, T. (2014), "Seismic optimum design of triple friction pendulum bearing subjected to near-fault pulse-like ground motions", *Struct. Multidiscip. O.*, **50**(4), 701-716.
- Nagarajaiah, S., Narasimhan, S. and Johnson, E. (2008), "Structural control benchmark problem: Phase ii—nonlinear smart base - isolated building subjected to near - fault earthquakes", *Struct. Control Health Monit.*, **15**(5), 653-656.
- Ramallo, J.C., Johnson, E.A. and Spencer Jr., B.F. (2002), " 'Smart' base isolation systems", *J. Eng. Mech.*, **128**(10), 1088-1099.
- Scruggs, J.T., Taflanidis, A.A. and Beck, J.L. (2006), "Reliability-based control optimization for active base isolation systems", *Struct. Control Health Monit.*, **13**(2-3), 705-723.
- Shan, J., Shi, Z., Hu, F., Yu, J. and Shi, W. (2018), "Stochastic optimal design of novel nonlinear base isolation system for seismic-excited building structures", *Struct. Control Health Monit.*, e2168. <https://doi.org/10.1002/stc.2168>
- Skinner, R.I., Robinson, W.H. and McVerry, G.H. (1993), An introduction to seismic isolation, John Wiley & Sons.
- Taghavi, S. and Miranda, E. (2003), Response assessment of nonstructural building elements, Pacific Earthquake Engineering Research Center.
- Yang, H.T.Y., Lin, C.H., Bridges, D. et al. (2010), "Bio-inspired passive actuator simulating an abalone shell mechanism for structural control", *Smart Mater. Struct.*, **19**(10), 105011.